

UCLA

UCLA Previously Published Works

Title

Common cerebral networks associated with distinct deep brain stimulation targets for cluster headache

Permalink

<https://escholarship.org/uc/item/3qc425cn>

Journal

Cephalalgia, 34(3)

ISSN

0333-1024

Authors

Clelland, Claire D
Zheng, Zhong
Kim, Won
[et al.](#)

Publication Date

2014-03-01

DOI

10.1177/0333102413509431

Peer reviewed



Published in final edited form as:

Cephalalgia. 2014 March ; 34(3): 224–230. doi:10.1177/0333102413509431.

Common cerebral networks associated with distinct deep brain stimulation targets for cluster headache

Claire D Clelland¹, Zhong Zheng¹, Won Kim¹, Ausaf Bari¹, and Nader Pouratian^{1,2,3,4}

¹Department of Neurosurgery, University of California, Los Angeles

²Department of Bioengineering, University of California, Los Angeles

³Neuroscience Interdepartmental Program, University of California, Los Angeles

⁴Brain Research Institute, University of California, Los Angeles

Abstract

Background—Several centers have reported efficacious cluster headache suppression with deep brain stimulation (DBS) of the hypothalamic region using a variety of targets. While the connectivity of some of these targets have individually been studied, commonalities across these targets, especially with respect to network-level connectivity, have not previously been explored.

Methods—We examined the anatomic connectivity of the four distinct DBS targets reported in the literature using probabilistic diffusion tensor tractography in normal subjects.

Results—Despite being described as hypothalamic, the DBS targets localized in the midbrain tegmentum posterior to the hypothalamus. Common tracts across DBS targets and subjects included projections to the ipsilateral hypothalamus, reticular formation and cerebellum.

Discussion—Although DBS target coordinates are not located within the hypothalamus, a strong connection between DBS targets and the hypothalamus likely exists. Moreover, a common projection to the medial ipsilateral cerebellum was identified. Understanding the common connectivity of DBS-targeted regions may elucidate anatomic pathways that are involved in modulating cluster headache attacks and facilitate more precise patient-specific targeting of DBS.

Keywords

cluster headache; deep brain stimulation; probabilistic tractography; hypothalamus; cerebellum

INTRODUCTION

Deep brain stimulation (DBS) has been reported to be effective in greater than 60% of patients implanted for treatment-refractory cluster headache (Table 1). DBS therapy has been targeted at the hypothalamic region based on neuroimaging studies that have

Corresponding Author: Nader Pouratian MD PhD, UCLA Neurosurgery, 10945 Le Conte Ave Suite 2120, Los Angeles, CA90095, 310-206-2189, FAX 310-794-1848, npouratian@mednet.ucla.edu.

CONFLICT OF INTEREST STATEMENT

The authors declare there is no conflict of interest.

implicated this region in cluster headache physiology. However, the precise region involved in cluster headache and therefore the presumed or optimal target for DBS is neither well understood nor characterized. The earliest landmark studies implicating the hypothalamic region in cluster headaches reported activation of the ipsilateral posterior hypothalamus during nitroglycerine-induced (1) and spontaneous (2) cluster attacks, an effect not seen during pain-free states. However, reanalysis of this data more precisely localizes the areas of activation to the midbrain tegmentum (3) and more recent fMRI data have shown activation of the posterior hypothalamus during cluster attacks, a region anterior and superior to that localized through PET (3, 4). Likewise, a recent series reexamining the coordinates used for therapeutic suppression of cluster headaches with DBS has shown that effective therapy is in fact achieved with modulation of the diencephalic-mesencephalic junction, a region posterior to the hypothalamus (5).

Although most reports refer to a “hypothalamic” target, the optimal targets reported by each series vary considerably and are generally not located within the anatomically-defined limits of the hypothalamus (Table 1). To date, commonalities across the reported targets have not been analyzed. Moreover, the anatomical circuitry underlying DBS’s efficacy in cluster headache is not well understood. In light of the increasingly accepted notion that DBS modulates neural networks rather than isolated targets, in this report we explore the commonalities in connectivity of the various reported efficacious DBS targets. We used reported efficacious DBS stereotactic coordinates to seed probabilistic magnetic resonance diffusion tractography in healthy subjects and examined the resultant pathways shared by these various targets. Understanding the common connectivity of DBS-targeted regions may elucidate anatomic pathways that are involved in modulating cluster headache attacks and facilitate more precise targeting of DBS on a patient-specific basis.

MATERIALS & METHODS

Subjects & Image Acquisition

Seven healthy subjects (6 male, 1 female) underwent imaging under a protocol approved by the UCLA Institutional Review Board. Ages ranged from 31 – 55 years (mean 44 years). Three of the patients were left-handed. T1-weighted axial and T2-weighted coronal MR images were obtained in a 3-Tesla machine (Siemens, Trio, Germany) as previously reported (6). T1-weighted axial (gradientecho; TR=11 ms TE=2.81 ms, matrix=256 × 256, whole brain, voxel size=0.9 × 0.9 × 0.9mm³) and T2-weighted coronal (turbo spin echo; TR=5000 ms, TE=62 ms, matrix 512 × 512, 18 slices centered on the hypothalamic region, voxel size=0.4 × 0.4 × 3mm³) A single-shot axial spin-echo echo-planar sequence was used for diffusion tensor imaging (DTI): b₀=1.000 s/mm², matrix=128 × 128, voxel size=2 × 2 × 2mm³ and diffusion gradients in 20 non-collinear directions (6).

Probabilistic tractography

Probabilistic diffusion tractography and image processing was performed using FSL tools (FMRIB’s Diffusion toolbox (FDT); <http://www.fmrib.ox.ac.uk/fsl>) in accordance with previously described methods (7). Briefly, before performing tractography, the eddy current correction tool within FSL was used to apply affine registrations to each volume in the

diffusion dataset to register it with the initial reference B0 volume. Skull stripping was performed using the brain extraction tool (BET). Voxel wise estimates of fiber orientations and their uncertainty, accounting for the possibility of crossing fibers within each voxel, were calculated using BEDPOSTX, with 2 fibers modeled per voxel, a multiplicative factor (i.e., weight) of 1 for the prior on the additional modeled fibers, and 1000 iterations before sampling (8). Eight “seed” masks (four per hemisphere) were created in each subject’s high-resolution T1-weighted structural space. Coordinates used were those previously reported (x, y, z calculated from the midpoint of the anterior commissure-posterior commissure line) $\pm 2, -3, -5; \pm 2, -6, -8$ (Table 1); mean coordinates of effective contacts as previously reported (5): $\pm 2.98, -3.53, -3.31$; and 4 mm from the 3rd ventricle wall, $-2, -5$ (9). Coordinates were transformed to diffusion space (using transformations defining the relationship between T1 and diffusion space as defined by FLIRT using 6 parameter transformation and mutual information) and used as a 2x2 mm voxel “seed” to determine the probabilistic tractography of each seed with the rest of the brain using PROBTRACKX (using 5000 samples, a 0.2 curvature threshold, and loopcheck termination).

Analysis of Tractography

In order to identify common tracts across seeds/targets and across subjects, we initially focused our analysis on the single subject level. For each subject, we generated two maps: a “single-subject common pathway map” (including voxels that contained projections from all 4 seeds/targets, generated by taking the product of the four within-subject projection maps and binarizing the result) and a “single-subject average projection map” (generated by averaging the projection maps of each of the 4 seeds/targets). Note that the single-subject average projection map is specifically generated to identify the average probability that a given voxel will be within the projection path of the targets. This is in distinction to a product map which would address the probability that all 4 targets within a subject simultaneously project to each voxel.

To generate an average projection map across all targets and across all subjects (“group average projection map”), all single-subject average projection maps were registered into MNI152 2mm standard space (FLIRT, 12 parameter) and averaged. Given that this map is a group average of individual average of probabilities across multiple targets without normalization, the group average projection map does not represent an average but a weighted illustrative representation of the distribution of projections across all subjects and all targets. To identify common pathways across all subjects and all targets (“group average common projection map”), in contrast to *average* pathways across all subjects and all targets, each single-subject common pathway map (which is a binarized single subject maps) was registered into MNI152 2mm standard space (FLIRT, 12-parameter) and averaged, resulting in a map of the frequency with which “single subject common pathway maps” involved each voxel in standard space. Therefore, to identify voxels that were part of the common pathway in at least 3 subjects, the “group average common projection map” was thresholded at 0.29 and binarized for illustrative purposes. To illustrate a relative probability of connectivity of each of these voxels with the four seeds/targets in question, the resultant binarized “group common projection map” was multiplied on a voxel-by-voxel basis with the “group average projection map.” The final output represents the pathways *across*

subjects common to all 4 seed/target regions with each voxel representing a hit by *at least* 3 subjects with color representing average probability of connectivity.

RESULTS

The stereotactic coordinates/targets used as seeds were localized in the gray matter of the midbrain tegmentum, posterior to the hypothalamus (Figure 1). The “group average projection map” (Figure 2) which illustrates the average projection of all targets across all subjects showed diffuse projections to ipsilateral frontal lobe (orbitofrontal regions), temporal lobe, hypothalamus, reticular formation, and cerebellum, with the strongest projections on average to the latter three structures. The “group average common projection map” (Figure 3A) illustrates in standard space how often a voxel in standard space was included in “single subject common pathway maps” and as expected demonstrates a similar pattern to that seen in Figure 2, with most subjects demonstrating common pathways projecting to ipsilateral hypothalamus, reticular formation, and cerebellum. When the “group average common projection map” was thresholded to only include common pathways that were present in at least 3 subjects, the resultant maps reinforces the observation of common connectivity to the ipsilateral hypothalamus, ipsilateral reticular formation, and the ipsilateral cerebellar cortex via the superior cerebellar peduncle (Figure 3B). As can be seen in Figure 3A, these projections to ipsilateral hypothalamus, ipsilateral reticular formation, and ipsilateral cerebellar cortex were robust and seen even when thresholding to identify those voxels present in at least 50% (4 of 7) subjects (represented by bright yellow and bright blue voxels in Figure 3A). Similar patterns of common projections were also observed when group data was thresholded to identify those voxels involved in projection pathways in at least 5 of 7 (71%) and 6 of 7 (86%) of subjects. These data represent the most stringent analysis of pathways common to all 4 targets, with the elimination of pathways present in fewer than three subjects. Of note, in addition to the common pathways shown in the group analysis (Figure 3B), one patient had additional pathways to the bilateral parietal and frontal cortices, which is depicted in Figure 2 representing an average of all pathways from the 4 target seeds without thresholding.

DISCUSSION

The justification for the anatomic coordinates used to target DBS electrode placement (Table 1) is based on early PET and MRI studies with limited spatial resolution in patients experiencing cluster attacks (1, 4, 10, 11). Whether the activation seen in these studies occurs in the posterior hypothalamus or the midbrain tegmentum has been debated (3). Using previously reported coordinates to create “seed” masks in our normal subjects, we confirm that these coordinates lie in the midbrain tegmentum gray matter adjacent to the third ventricle, posterior to the hypothalamus, a region that is hypothesized to be part of a pain network (5, 9). Imprecise localization of electrodes based on poorly-understood circuitry or individual anatomic variation may in part account for the 30–40% of cluster headache patients (Table 1) for whom DBS is ineffective.

The mechanisms of neuromodulation and the anatomical underpinnings of effective DBS in cluster headache are not known. One important question is whether a local effect or distant

neuromodulation underlies the effectiveness of electrical stimulation. We report three major regions of connectivity common to all seed coordinates evaluated: the ipsilateral hypothalamus, reticular formation, and cerebellar hemisphere. Given that it is currently not possible to differentiate directionality using DTI, we cannot determine whether these data represent one pathway projecting from the hypothalamus through the seed regions to the cerebellum, or vice versa, although the pattern of connectivity is suggestive of such a pathway.

The posterior hypothalamus has been hypothesized to play a pivotal role in initiating cluster headaches owing to the periodicity of attacks, neuroendocrine alterations in patients with cluster headache (12), and purported hypothalamic PET and fMRI activation during cluster attacks (1, 2, 4). Conversely, a larger “pain matrix” in which the hypothalamus plays a role may be responsible for modulating cluster headache attacks, a hypothesis in agreement with diffuse activation during imaging of cluster attacks (1, 2, 4, 9, 13).

DTI probabilistic tractography in humans (6) has suggested a direct connection between the hypothalamus and cerebellum. Interestingly, PET (1, 14) and MRI (4, 13) studies have shown activation of both the ipsilateral hypothalamus and cerebellum in patients during cluster attacks, regions that are not activated in pain-free states. Furthermore, in patients with chronic cluster headache implanted with DBS electrodes, the cerebellum has enhanced 15-O-H₂O PET activity during stimulator-on states compared to stimulator-off states (15) and chronic occipital nerve stimulation modulates cerebellar 18-FDG PET hyperactivation in cluster headache patients (14). Whether the cerebellum plays a direct role in modulating cluster headache is not known, although cerebellar activation has been suggested to play an active role in pain modulation (16) and may be part of a larger “pain matrix” (9).

Interestingly, our data align with data by Seijo *et al.* (9) which showed projections between DBS electrode target sites and the ipsilateral cerebellum in two patients with cluster headache using diffusion tensor tractography. Unlike Owen *et al.* (17), however, we do not show projections to parietal or frontal cortices as a pathway common to all seeded regions across patients. Although these pathways were present in unthresholded preliminary analyses (Figure 2), the more stringent treatment of diffusion data in this analysis eliminated pathways to these regions observed in one patient in our pooled analysis. This is consistent with both Owen *et al.*'s (17) and Seijo *et al.*'s (9) reports and figures that connections to the cerebellum and the reticular nucleus are much more robust. One should consider, however, that differences in studies may in part be due to limitations in the spatial resolution of DTI analysis and that DTI data with the spatial resolution used in this study (2mm) may not completely account for differences in connectivity of all the targets studied.

By seeding DBS-target regions in diffusion tensor imaging, we show connectivity with the hypothalamus and cerebellum common to all DBS targets probed in normal subjects. Our data also suggest that tractography could be used to facilitate surgical planning, utilizing a pathway approach within patients to localize more precise anatomic targets. Despite grossly normal structural imaging in patients with cluster headache, subtle differences in brain structure (as suggested by May *et al.* (11)) or aberrant connectivity may underlie cluster headache attacks. Therefore, confirmation of the current findings in patients who have

undergone effective DBS compared to patients for whom DBS is ineffective would elegantly address questions our current data raise regarding the pathways that are critical for cluster headaches and may suggest new targets for future surgical intervention.

Acknowledgments

FUNDING

This work is supported by funds provided by National Institute of Biomedical Imaging and Bioengineering under Award Number K23EB014326 (N.P.) and the UCLA Department of Neurosurgery Visionary Ball. We would like to thank the Jack Kent Cooke Foundation for its support of author CDC.

References

1. May A, Bahra A, Buchel C, Frackowiak RS, Goadsby PJ. Hypothalamic activation in cluster headache attacks. *Lancet*. 1998; 352:275–8. [PubMed: 9690407]
2. Sprenger T, Boecker H, Tolle TR, Bussone G, May A, Leone M. Specific hypothalamic activation during a spontaneous cluster headache attack. *Neurology*. 2004; 62:516–7. [PubMed: 14872051]
3. Matharu MS, Zrinzo L. Deep brain stimulation in cluster headache: hypothalamus or midbrain tegmentum? *Curr Pain Headache Rep*. 14:151–9. [PubMed: 20425205]
4. Morelli N, Pesaresi I, Cafforio G, Maluccio MR, Gori S, Di Salle F, Murri L. Functional magnetic resonance imaging in episodic cluster headache. *J Headache Pain*. 2009; 10:11–4. [PubMed: 19083151]
5. Fontaine D, Lanteri-Minet M, Ouchchane L, Lazorthes Y, Mertens P, Blond S, et al. Anatomical location of effective deep brain stimulation electrodes in chronic cluster headache. *Brain*. 133:1214–23. [PubMed: 20237130]
6. Lemaire JJ, Frew AJ, McArthur D, Gorgulho AA, Alger JR, Salomon N, et al. White matter connectivity of human hypothalamus. *Brain Res*. 1371:43–64. [PubMed: 21122799]
7. Pouratian N, Zheng Z, Bari AA, Behnke E, Elias WJ, Desalles AA. Multi-institutional evaluation of deep brain stimulation targeting using probabilistic connectivity-based thalamic segmentation. *J Neurosurg*. 115:995–1004. [PubMed: 21854118]
8. Behrens TE, Berg HJ, Jbabdi S, Rushworth MF, Woolrich MW. Probabilistic diffusion tractography with multiple fibre orientations: What can we gain? *Neuroimage*. 2007; 34:144–55. [PubMed: 17070705]
9. Seijo F, Saiz A, Lozano B, Santamarta E, Alvarez-Vega M, Seijo E, et al. Neuromodulation of the posterolateral hypothalamus for the treatment of chronic refractory cluster headache: Experience in five patients with a modified anatomical target. *Cephalalgia*. 31:1634–41. [PubMed: 22116943]
10. Leone M, Franzini A, Bussone G. Stereotactic stimulation of posterior hypothalamic gray matter in a patient with intractable cluster headache. *N Engl J Med*. 2001; 345:1428–9. [PubMed: 11794190]
11. May A, Ashburner J, Buchel C, McGonigle DJ, Friston KJ, Frackowiak RS, Goadsby PJ. Correlation between structural and functional changes in brain in an idiopathic headache syndrome. *Nat Med*. 1999; 5:836–8. [PubMed: 10395332]
12. Leone M, Bussone G. A review of hormonal findings in cluster headache. Evidence for hypothalamic involvement. *Cephalalgia*. 1993; 13:309–17. [PubMed: 8242722]
13. Teepker M, Menzler K, Belke M, Heverhagen JT, Voelker M, Mylius V, et al. Diffusion tensor imaging in episodic cluster headache. *Headache*. 52:274–82. [PubMed: 22082475]
14. Magis D, Bruno MA, Fumal A, Gerardy PY, Hustinx R, Laureys S, Schoenen J. Central modulation in cluster headache patients treated with occipital nerve stimulation: an FDG-PET study. *BMC Neurol*. 11:25. [PubMed: 21349186]
15. May A, Leone M, Boecker H, Sprenger T, Juergens T, Bussone G, Tolle TR. Hypothalamic deep brain stimulation in positron emission tomography. *J Neurosci*. 2006; 26:3589–93. [PubMed: 16571767]

16. Helmchen C, Mohr C, Erdmann C, Binkofski F. Cerebellar neural responses related to actively and passively applied noxious thermal stimulation in human subjects: a parametric fMRI study. *Neurosci Lett*. 2004; 361:237–40. [PubMed: 15135937]
17. Owen SL, Green AL, Davies P, Stein JF, Aziz TZ, Behrens T, et al. Connectivity of an effective hypothalamic surgical target for cluster headache. *J Clin Neurosci*. 2007; 14:955–60. [PubMed: 17689083]
18. Schoenen J, Di Clemente L, Vandenhede M, Fumal A, De Pasqua V, Mouchamps M, et al. Hypothalamic stimulation in chronic cluster headache: a pilot study of efficacy and mode of action. *Brain*. 2005; 128:940–7. [PubMed: 15689358]
19. Leone M, Franzini A, Broggi G, Bussone G. Hypothalamic stimulation for intractable cluster headache: long-term experience. *Neurology*. 2006; 67:150–2. [PubMed: 16832097]
20. Starr PA, Barbaro NM, Raskin NH, Ostrem JL. Chronic stimulation of the posterior hypothalamic region for cluster headache: technique and 1-year results in four patients. *J Neurosurg*. 2007; 106:999–1005. [PubMed: 17564171]
21. Bartsch T, Pinsker MO, Rasche D, Kinfe T, Hertel F, Diener HC, et al. Hypothalamic deep brain stimulation for cluster headache: experience from a new multicase series. *Cephalalgia*. 2008; 28:285–95. [PubMed: 18254897]
22. Brittain JS, Green AL, Jenkinson N, Ray NJ, Holland P, Stein JF, et al. Local field potentials reveal a distinctive neural signature of cluster headache in the hypothalamus. *Cephalalgia*. 2009; 29:1165–73. [PubMed: 19366355]
23. Fontaine D, Lazorthes Y, Mertens P, Blond S, Geraud G, Fabre N, et al. Safety and efficacy of deep brain stimulation in refractory cluster headache: a randomized placebo-controlled double-blind trial followed by a 1-year open extension. *J Headache Pain*. 11:23–31. [PubMed: 19936616]
24. Franzini A, Cordella R, Messina G, Marras CE, Romito LM, Albanese A, et al. Targeting the brain: considerations in 332 consecutive patients treated by deep brain stimulation (DBS) for severe neurological diseases. *Neurol Sci*.

ARTICLE HIGHLIGHTS

1. Reported DBS targets for treatment of cluster headache localize to the midbrain tegmentum rather than the hypothalamus.
2. DBS targets demonstrate robust structural connections with the hypothalamus, ipsilateral reticular formation, and medial ipsilateral cerebellum.
3. Frontal projections, as reported by others, are not common to all reported efficacious DBS targets.
4. These common patterns of structural connectivity across DBS targets may elucidate anatomic pathways that are involved in modulating cluster headache attacks and facilitate more precise patient-specific targeting.

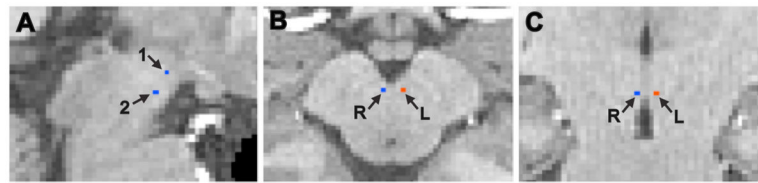


Figure 1.

Placement of stereotactic DBS cluster headache “seed” targets on normal subject’s T1-weighted MRI image. Sagittal image (A) of right hemisphere showing target 1 ($\pm 2, -3, -5$ from midcommissural point) and target 2 ($\pm 2, -6, -8$), both located in the midbrain tegmentum. The third ($\pm 2.98, -3.53, -3.31$) and fourth (4 mm from the 3rd ventricle wall, $-2, -5$) targets are outside of the plane of the image. Target 1 is also depicted on axial (B) and coronal (C) sections in the left and right hemispheres.

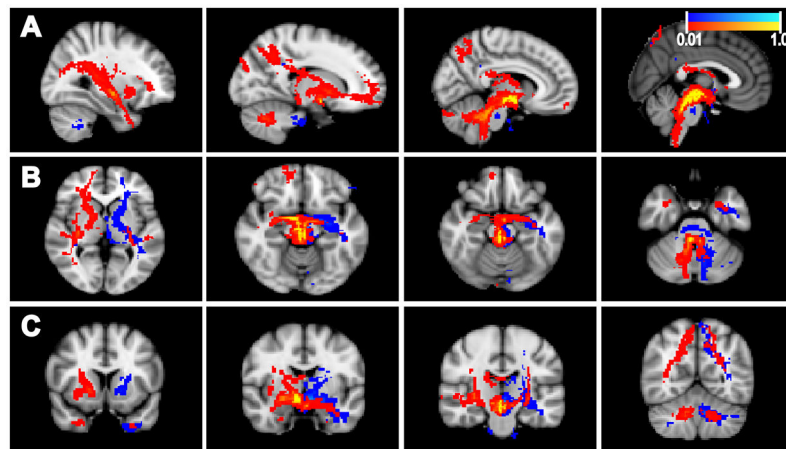


Figure 2.

Group Average Projection Map. Average single-subject projection maps of 4 stereotactic DBS cluster headache “seed” targets across normal subjects (n=7) without thresholding overlaid on a standard structural brain image. Pathways projected to the ipsilateral frontal lobe (orbitofrontal cortex) (axial view/panel B), temporal lobe (sagittal view/panel A), hypothalamus and reticular formations (panel B and coronal view/panel C), and the cerebellum (panels A and C). The strongest common projections were to the hypothalamus, reticular formation, and cerebellum (yellow color). Scale bar represents probability of a pathway passing through a voxel (probability of 1 is depicted in yellow for right hemisphere seeds and light blue for left hemisphere seeds).

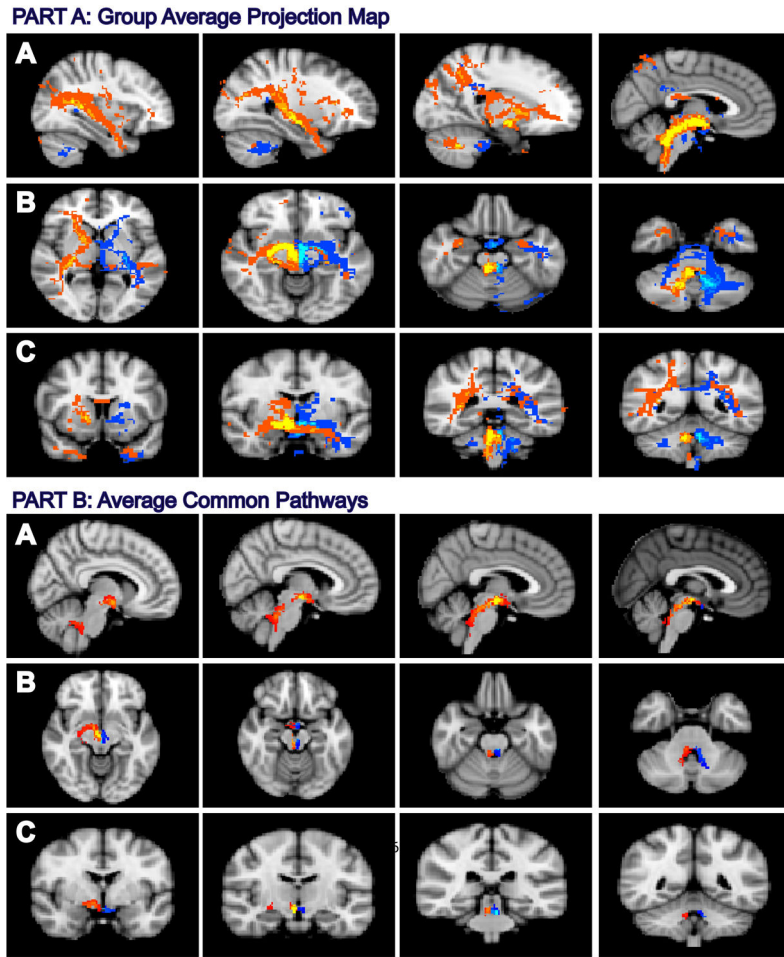


Figure 3.

Average Common Pathways Across Subjects. Group average common projection map (panels A1-3) of 4 stereotactic DBS cluster headache “seed” targets across normal subjects ($n=7$) illustrates in standard space the frequency by which each voxel was included in “single subject common pathway maps.” The pattern is similar to that of Figure 2, with most subjects demonstrating common pathways projecting to the ipsilateral hypothalamus, reticular formation, and cerebellum (yellow and light blue colors, panels A1-3). Note, solid yellow and light blue regions represent voxels involved in at least 50% of subjects. Average common pathways across subjects (panels B1-3) represents pathways present in all 4 DBS “seed” target projection maps and at least 3 subjects (thresholded data from panels A1-3). Common pathways projected to the ipsilateral hypothalamus, ipsilateral reticular formation, and the ipsilateral cerebellar cortex via the superior cerebellar peduncle (yellow and light blue colors, panels A1-3). Scale bar, panels B1-3 represents probability of a pathway passing through a voxel across targets and subjects (probability of 1 is depicted in yellow for right hemisphere seeds and light blue for left hemisphere seeds).

Table 1

Reported DBS cases and stereotactic coordinates in chronic cluster headache

Authors & Year	Number of Patients	Stereotactic coordinates (x, y, z, from midcommissural point)	Mean Follow-up (years)	Number of Responders	% of patients improved (decrease in weekly frequency of attacks > 50%)
Leone <i>et al.</i> 2001 (10)	1	$\pm 2, -6, -8$	1	1	100
Schoenen <i>et al.</i> 2005 (18)	4	$\pm 2, -6, -8$	1.2	2	50
Leone <i>et al.</i> 2006 (19)	16	$\pm 2, -3, -5$	4	13	81
Starr <i>et al.</i> 2007 (20)	4	$\pm 2, -3, -5$	1	2	50
Bartsch <i>et al.</i> 2008 (21)	6	$\pm 2, -3, -5$	1.4	3	50
Brittain <i>et al.</i> 2009 (22)	2	$\pm 2, -6, -8$	0.8	2	100
Fontaine <i>et al.</i> 2010 (23)	11	$\pm 2, -3, -5$	1	6	55
Seijo <i>et al.</i> 2011 (9)	5	4 mm from 3 rd ventricle wall, $-2, -5$	2.7	5	100
Frazzini <i>et al.</i> 2012 (24)	22	$\pm 2, -3, -5$	8	14	63